



International Symposium on Imaging, Sensing, and Optical Memory (ISOM' 21), Kobe, Japan

# Fabrication of ITO diffraction grating structure for infrared plasmonics by thermal nanoimprint lithography

Noriyuki Hasuike<sup>1</sup> · Takeshi Maeda<sup>1</sup> · Minoru Takeda<sup>1</sup>

Received: 21 February 2022 / Accepted: 15 August 2022 / Published online: 30 August 2022  
© The Optical Society of Japan 2022

## Abstract

Indium tin oxide (ITO) diffraction grating was fabricated on a polyimide (PI) film by using a combination of thermal nanoimprint lithography (NIL) process and radio frequency (RF) sputtering method. The thermal NIL process was used to transfer a line and space pattern to the PI film and then an ITO thin film with a thickness of several hundred nanometers was deposited on the patterned PI film. A polarized reflection spectrum showed a characteristic decrease in reflectance due to surface plasmon resonance in an infrared spectral region, which is similar to that of the grating fabricated directly on ITO film using focused ion beam lithography. The fabrication process proposed in this study can easily realize an ITO grating structure with a large area.

**Keywords** Surface plasmon resonance · ITO · Diffraction grating · Thermal nanoimprint lithography

## 1 Introduction

Surface nanostructures cause materials to develop unique optical properties in addition to their original characteristics. They enable the realization of new optical devices that transcend conventional optical technologies and they are a key technology in the fields of nanophotonics and plasmonics. Nanostructures are often fabricated using semiconductor fine-processing technology, such as photolithography, electron beam lithography (EBL), and focused ion beam (FIB) lithography. These techniques have enabled the fabrication of ultrafine structures with high precision; however, they require a high-investment in facilities and a time-consuming process to fabricate them in a large area.

Recently, a nonconventional lithographic technique is known as nanoimprint lithography (NIL) has attracted attention as a high-throughput nanopatterning technique, and it is expected as a new processing method for semiconductor processing and optical device applications. NIL is a

technique for transferring nanopatterns to polymer substrates by impressing the mold with desired patterns. This technique is useful for industrial applications because it allows the fabrication of surface nanostructures on large substrates at low cost and high speed [1–4]. Additionally, it has a significant advantage in advancing nanophotonics and plasmonics research in small laboratories.

Plasmonic behaviors are often observed on metal nanostructures such as Au and Ag, but recently, indium tin oxide (ITO) nanostructures, such as nanoparticle-sheet [5], nanorod-array [6, 7], and disk resonator array [8] have attracted much attention as plasmonic materials working in the infrared spectral region. These applications contribute to the development of energy-saving technology and the improvement of bio-sensing sensitivity, and it will be one of the remarkable research fields for the realization of a sustainable society in the future. In addition, ITO-based plasmonic materials have the unique feature that the surface plasmon resonance (SPR) wavelength can be modulated by electric properties that can be tuned by the doping level and the density of oxygen vacancies [9–12].

We previously reported on the excitation of SPR in ITO films using a diffraction grating coupler and found that SPR can be excited by incident of *p* - polarized light to the ITO grating coupler, and the resonant wavelength roughly

✉ Noriyuki Hasuike  
hasuike@kit.ac.jp

<sup>1</sup> Department of Electronics, Kyoto Institute of Technology, Matsugasaki, Kyoto, Sakyo-ku 606-8585, Japan

depends on both the grating pitch [13] and the electric properties [14].

In this study, we propose a new process for fabricating ITO gratings that combines the thermal NIL process with radio frequency (RF) sputtering method. It is simpler than the conventional FIB process and can be used to prepare an ITO grating in a large area at a low cost.

So far, ITO nanostructured films prepared on a substrate patterned using NIL have been reported. Brigo et al. fabricated ITO two-dimensional (2D) gratings by using a solution process and NIL [15]. Although they discussed its far-field optical properties, they do not mention the plasmonic properties of the ITO 2D grating. They describe the goal as realizing a 2D plasmonic crystal using the ITO 2D grating as a template layer and depositing a metal thin film on it. Additionally, Lee et al. have succeeded in driving a liquid crystal using ITO nanostructured thin film with high transparency and electrical conductivity similar to the one used by Brigo et al. [16]. However, they do not evaluate the plasmonic optical properties. In these studies, ITO nanostructures were successfully fabricated and demonstrated good optical properties for their application, but the fabrication method was different from ours.

However, Khan et al. have fabricated ITO transparent electrode with a 2D corrugated surface by combining UV-NIL and sputtering deposition, which is similar to our method [17]. They were successful in realizing an ITO electrode with higher transparency than the conventional one by efficiently using plasmonic properties due to ITO 2D corrugated surface. However, the plasmonic properties of the ITO corrugated surface are not evaluated in detail.

In this study, we focused on the evaluation of plasmonic properties due to SPR on ITO nanograting fabricated by combining NIL and sputtering deposition. We establish experimentally that an ITO grating fabricated by combining NIL and sputter deposition exhibits the same surface plasmon characteristics as a conventional one fabricated directly on ITO bulk film.

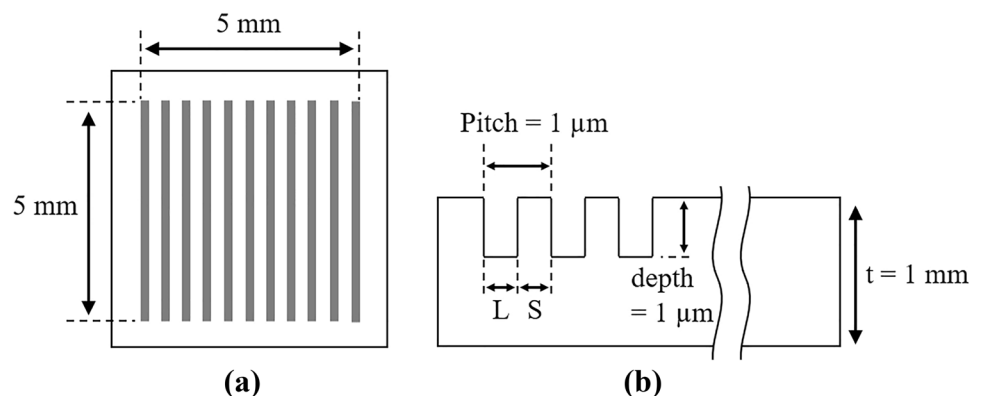
## 2 Imprinting of grating pattern

Thermal NIL was used to imprint a grating pattern on a 200  $\mu\text{m}$  thickness thermoplastic polyimide (PI) film. A Commercially-supplied Si mold with a line (L) and space (S) pattern ( $L/S=1:1$ ) and a depth of 1  $\mu\text{m}$  was used for imprinting mold. The illustration is shown in Fig. 1. The mold is ultrasonically cleaned in distilled water and ethanol before running the imprint process and then introduced into an oxygen plasma ashing device to remove organic contaminants adhering to the surface. Subsequently, the mold surface was treated with perfluoropolyether (PFPE) containing a silane coupling agent for anti-sticking and easy mold release after imprinting. The mold release agent is available as OPTOOL (DAIKIN Co., Ltd., Osaka).

The thermal NIL process proceeds according to the process sequence shown in Fig. 2. First, PI film is heated up to preset temperature  $T_p$  for 20 s to soften, and after that, loading force is gradually applied until it reaches preset value  $P_p$  and is maintained for 100 s.  $T_p$  and  $P_p$  values are varied in the range of 260 ~ 290  $^\circ\text{C}$  and 0.6 ~ 1.9 MPa, respectively. The PI film and mold are then cooled by applying a loading force in tens of seconds to form a transferred pattern. Finally, the mold is removed from the PI film.

Figure 3a ~ (d) show plan SEM images of the patterned PI film. Plan views showed L and S patterns with a pitch of approximately 1  $\mu\text{m}$  corresponding to the pitch of the mold for all samples. However, the L and S ratio in the sample prepared at 260  $^\circ\text{C}$  did not agree with that of the mold (1:1). The structure of the transferred pattern was investigated in detail using cross-sectional SEM observation. The images are shown in Fig. 3(e) ~ (h). The samples for cross-sectional observation were prepared by exposing the smooth surface with FIB after cutting the film with a thin and sharp metal blade. The grating in the sample prepared at 260  $^\circ\text{C}$  and 0.6 MPa had a shape with rounded corners and the depth was shallower than that of the mold, approximately estimated at 0.3  $\mu\text{m}$ .

**Fig. 1** **a** Plan and **b** cross-sectional illustration of Si mold



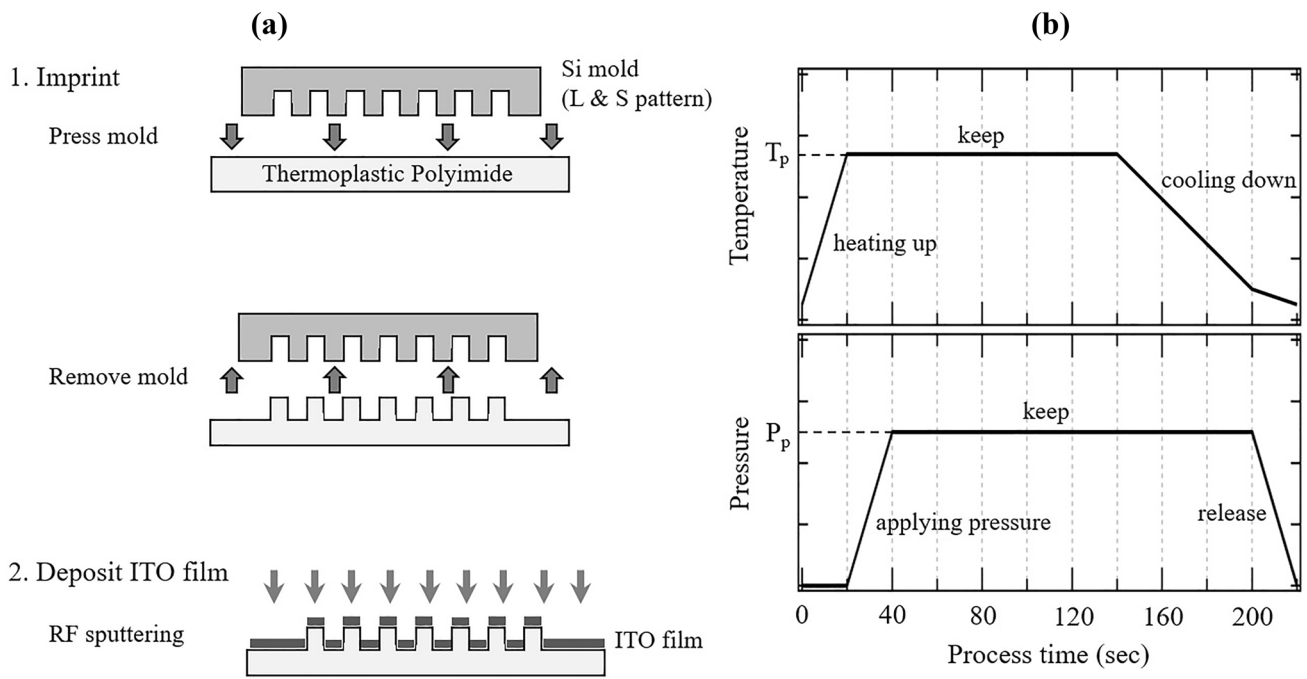
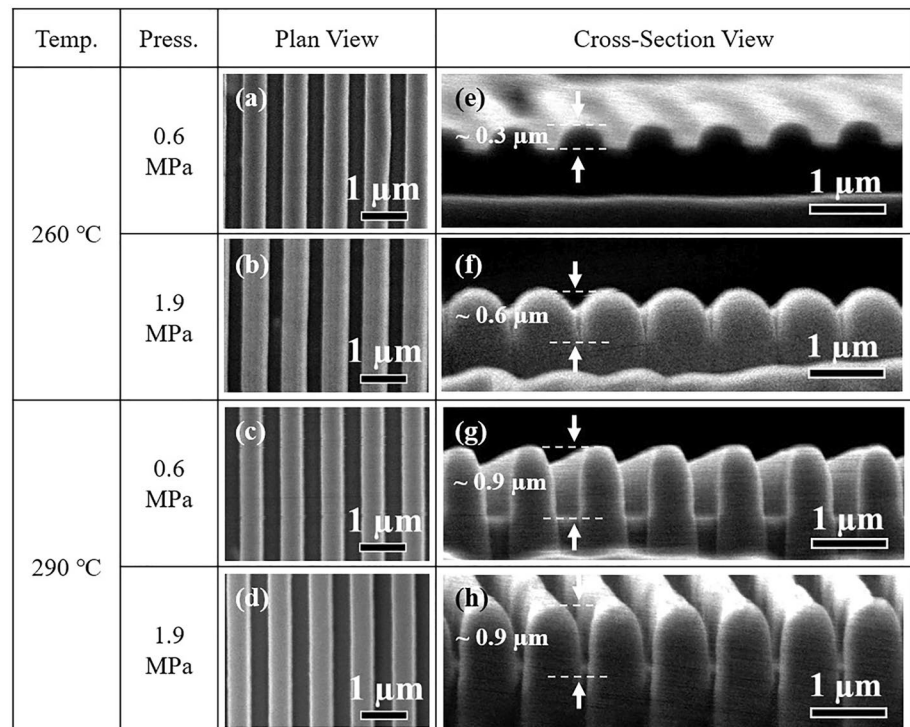


**Fig. 2** Illustration of NIL and ITO deposition sequence (a) and preset parameters (b)

**Fig. 3** Plan SEM images (a)–(d) and cross-sectional SEM images (e)–(h) of the samples imprinted under different conditions



Although the depth increased slightly as the loading force increased up to 1.9 MPa, it still did not agree with the mold. Regardless of the imprinting pressure, the mold pattern was well-transferred in the sample prepared at

290 °C. This is because the glass transition temperature of PI is approximately 300 °C, and it becomes softer at that temperature.

### 3 ITO diffraction grating

#### 3.1 ITO deposition on patterned PI film

ITO films were deposited using the RF sputtering method at 250 °C on a patterned PI film prepared using thermal NIL at 290 °C and 1.9 MPa. The sputtering process was performed as follows; Ar gas was introduced into the sputtering chamber and the pressure was maintained at 0.3 Pa during the sputtering process. In<sub>2</sub>O<sub>3</sub> - SnO<sub>2</sub>(90:10 wt%) ceramics were used as a sputtering target and 100 W RF power was applied to the target.

Figure 4a and b show plain and cross-sectional SEM images of the sample deposited ITO for 1.5 h, respectively. The L and S patterns were well-maintained even after ITO deposition, but the S width became narrower.

The cross-sectional SEM observations shown in 4b clarified this change. With a thickness of 300 nm, an ITO film was uniformly deposited on both the top and side walls of the grating structure.

#### 3.2 SPR in ITO/PI diffraction grating

SPR excitation can be realized by an incident of *p*-polarized light on the grating, resulting in a characteristic decrease in reflectance as a dip on the reflection spectrum at the resonant wavelength.

Figure 5a shows the polarized reflection spectra of ITO/PI grating deposited ITO. The figure also includes an unpolarized spectrum taken from the sample’s surface (not grating). The plasma frequency  $\omega_p$  and the damping constant  $\Gamma$  were estimated from the free-carrier plasma reflection edge using Drude fitting analysis. These values give  $\omega_{SPR} - k_{SPR}$

**Fig. 4** Plan-view (a) and cross-sectional view (b) of the sample deposited ITO on patterned PI film

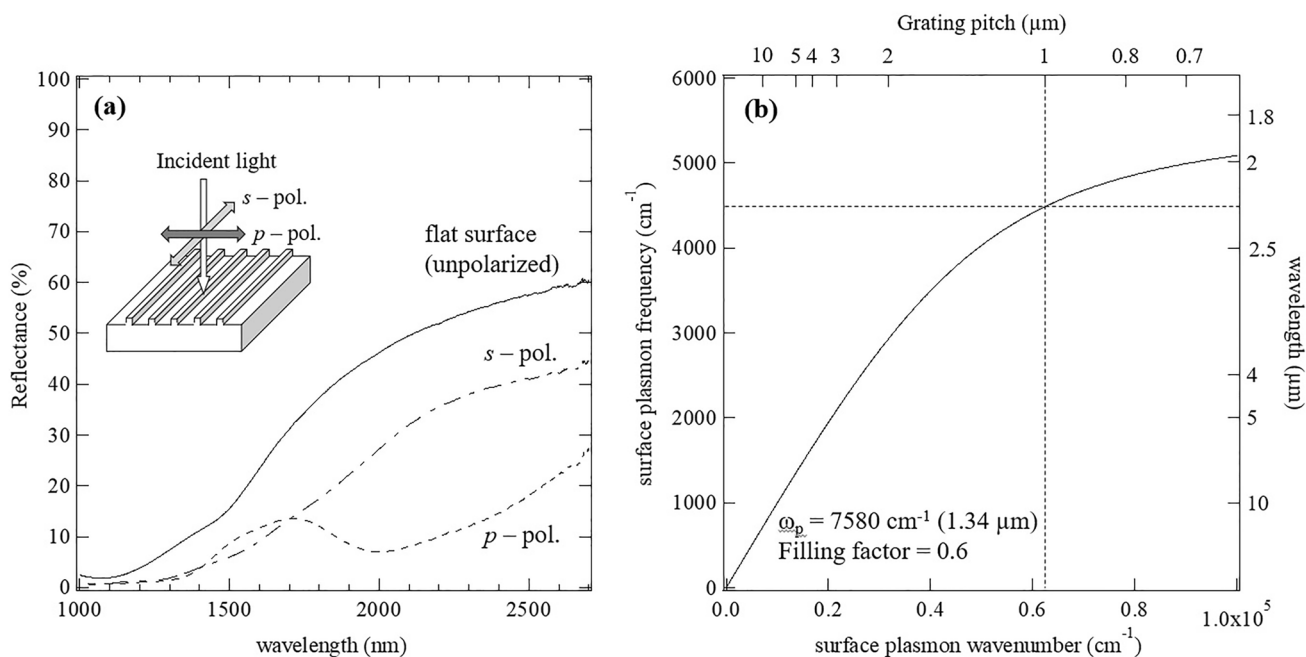
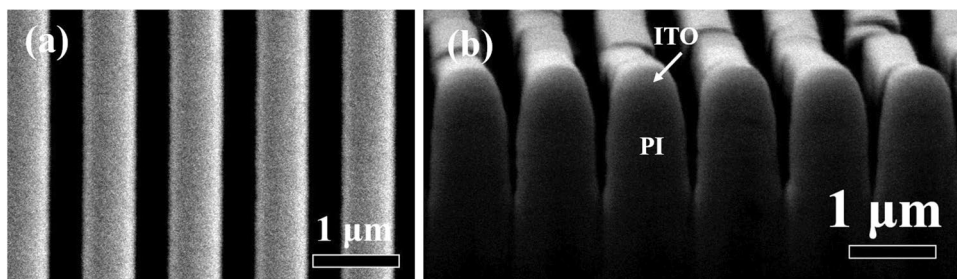


**Fig. 5** a Unpolarized and *p*-, *s*-polarized reflection spectra taken from flat surface and the ITO/PI grating, respectively. The inset shows the polarization direction of the incident light. b  $\omega_{SPR} - k_{SPR}$  dispersion relation on surface plasmon calculated using plasma fre-

quency  $\omega_p = 7580 \text{ cm}^{-1}$  and filling factor  $f = a/\Lambda = 0.6$ . Vertical and horizontal dotted line represent the grating pitch of the sample and predicted SPR wavelength

dispersion relation on propagating surface plasmon and it enables us to predict SPR wavelength. When SPR is excited at the interface between two types of a medium having complex dielectric constant  $\tilde{\epsilon}_1$  and  $\tilde{\epsilon}_2$ , the dispersion relation between SPR frequency  $\omega_{\text{SPR}}$  and SPR wavenumber  $k_{\text{SPR}}$  is given by the following equation;

$$k_{\text{SPR}} = \frac{\omega_{\text{SPR}}}{c} \left\{ \frac{\tilde{\epsilon}_1 \cdot \tilde{\epsilon}_2}{\tilde{\epsilon}_1 + \tilde{\epsilon}_2} \right\}^{\frac{1}{2}} \quad (1)$$

For SPR excited at the interface between ITO and air, the formula can be rewritten as follows using a complex dielectric constant of ITO ( $\tilde{\epsilon}_{\text{ITO}} = \epsilon'_{\text{ITO}} + i\epsilon''_{\text{ITO}}$ ) and air ( $\tilde{\epsilon}_{\text{air}} = 1$ );

$$k_{\text{SPR}} = \frac{\omega_{\text{SPR}}}{c} \left( \frac{\epsilon'_{\text{ITO}}}{\epsilon'_{\text{ITO}} + 1} \right)^{\frac{1}{2}} \quad (2)$$

$\epsilon'_{\text{ITO}}$  is given by the Drude model as follows.

$$\epsilon'_{\text{ITO}} = \epsilon_{\text{opt}} \left( 1 - \frac{\omega_p^2}{\omega^2 + \Gamma^2} \right) \quad (3)$$

From these equations, the dispersion relation can be calculated using  $\omega_p$  and  $\Gamma$ . The details are described in reference [14].

In this study,  $\omega_p$  and  $\Gamma$  were estimated at  $7580 \text{ cm}^{-1}$  by applying Drude fitting to the unpolarized spectrum. Additionally, the grating pitch  $\Lambda$  and the filling factor  $f = a/\Lambda$  ( $a$  is  $L$  width of the grating), which is required to calculate the SPR wavelength according to effective medium theory [14], were estimated at  $1 \mu\text{m}$  and  $0.6$  from SEM observation shown in Fig. 4a. With these values,  $\omega_{\text{SPR}} - k_{\text{SPR}}$  dispersion relation on propagating surface plasmon was obtained (Fig. 5b), and the SPR wavelength was predicted to be  $2.2 \mu\text{m}$ , as indicated by vertical and horizontal dotted lines. The  $p$ -polarized spectrum showed a characteristic decrease in reflectance from  $2.0 \mu\text{m}$  to a longer wavelength side compared with the  $s$ -polarized spectrum. The SPR excitation can be realized using a prepared ITO/PI grating, which corresponded well with previous work [14].

## 4 Conclusion

An ITO diffraction grating structure was successfully fabricated on a patterned PI film with a large area of several tens of  $\text{mm}^2$  using the combination of the thermal NIL process and RF sputtering method. The fabricated ITO/PI grating exhibited similar plasmonic properties to those obtained in a previous work, in which the grating was fabricated by FIB within a narrow area of several hundreds of  $\mu\text{m}^2$ . The technique proposed in this study is useful for the fabrication of large-area plasmonic nanostructures at a low

cost, and it is expected to be applied to various plasmonic materials and structures in the future.

## References

1. Elisa, M., Di Francesca, B., Luana, P., Roberto, C., Dario, P.: Multilevel, room-temperature nanoimprint lithography for conjugated polymer-based photonics. *Nano Lett.* **5**, 1915 (2005)
2. Pelloquin, S., Augé, S., Sharshavina, K., Doucet, J.-B., Hélot, A., Camon, H., Monmayrant, A., Gauthier-Lafaya, O.: Soft mold Nanoimprint Lithography: a versatile tool for sub-wavelength grating applications. *Microsyst. Technol.* <https://doi.org/10.1007/s00542-018-3740-6> (2018)
3. Kim, K., Yoon, Gwanho., Back, S., Rho, J., Lee, H.: Facile nanocasting of dielectric metasurfaces with sub-100 nm resolution. *ACS Appl. Mater. Interfaces* **11**, 26109 (2019)
4. Takeda, M., Takahara, R., Hasuike, N.: Plasmonic color pixels fabricated by nanoimprint process. *Opt. Rev.* **27**, 427 (2020)
5. Matsui, H., Hasebe, T., Hasuike, N., Tabata, H.: Plasmonic heat shielding in the infrared range using oxide semiconductor nanoparticles based on Sn-doped  $\text{In}_2\text{O}_3$ : effect of size and interparticle gap. *ACS Appl. Nano Mater.* **1**, 1863 (2018)
6. Li., S.Q., Guo, P., Zhang L., Zhou, W., Odom, Teri W., Seideman, Tamar., Ketterson, John B., Chang, Robert P. H.: Infrared plasmonics with indium-tin-oxide nanorod arrays. *ACS Nano* **5**, 9161 (2011)
7. Chen, K., Guo, P., Dao, D., Li, S.-Q., Ishii, S., Nagao, T., Chang, R.P.H.: Protein-functionalized indium-tin oxide nanoantenna arrays for selective infrared biosensing. *Adv. Opt. Mater.* **5**, 1700091 (2017)
8. Dao, T.D., Doan, A.T., Ngo, D.H., Chen, K., Ishii, S., Tamakai, A., Nagao, T.: Selective thermal emitters with infrared plasmonic indium tin oxide working in the atmosphere. *Opt. Mater. Exp.* **9**, 2534 (2019)
9. Kanehara, M., Koike, H., Yoshinaga, T., Teranishi, T.: Indium tin oxide nanoparticles with compositionally tunable surface plasmon resonance frequencies in the near-IR region. *J. Am. Chem. Soc.* **131**, 17736 (2009)
10. Matsui, H., Furuta, S., Tabata, H.: Role of electron carriers on local surface plasmon resonances in doped oxide semiconductor nanocrystals. *Appl. Phys. Lett.* **104**, 211903 (2014)
11. Losego, M.D., Efremenko, A.Y., Rhodes, C.L., Cerruti, M.G., Franzen, S., Maria, J.-P.: Conductive oxide thin films: model systems for understanding and controlling surface plasmon resonance. *J. Appl. Phys.* **106**, 024903 (2009)
12. Garcia, G., Buonsanti, R., Runnerstrom, E.L., Mendelsberg, R.J., Llordes, A.A., Richardson, T.J., Milliron, D.J.: Dynamically modulating the surface plasmon resonance of doped semiconductor nanocrystals. *Nano Lett.* **11**, 4415 (2011)
13. Hasuike, N., Ochiai, S., Iwakiri, R., Takeda, M., Yoo, W.S., Isshiki, T.: Surface plasmon resonances in Sn:  $\text{In}_2\text{O}_3$  thin films with diffraction grating. *MDPI Proc.* **2**, 1034 (2018)
14. Hasuike, N., Miyamoto, N., Funahashi, K., Takeda, M.: The correlation between electrical properties and surface plasmonic properties on ITO films with diffraction grating. *Opt. Rev.* **28**, 620 (2021)
15. Brigo, L., Mattei, G., Michieli, N., Brusatinm, G.: 2D photonic gratings from thermal imprinting of ITO-based films. *Microelectron. Eng.* **97**, 193 (2012)
16. Lee, S.H., Ha, N.Y.: Nanostructured indium-tin-oxide films fabricated by all-solution processing for functional transparent electrodes. *Opt. Exp.* **19**, 21803 (2011)

17. Khan, I., Bauch, M., Dimopoulos, T., Dostalek, J.: Nanostructured as-deposited indium tin oxide thin films for broadband antireflection and light trapping. *Nanotechnology* **28**, 325201 (2017)

Springer Nature or its licensor holds exclusive rights to this article under a publishing agreement with the author(s) or other rightsholder(s); author self-archiving of the accepted manuscript version of this article is solely governed by the terms of such publishing agreement and applicable law.